ITC 1/52
Information Technology and Control
Vol. 52 / No. 1 / 2023
pp. 228-244
DOI 10.5755/j01.itc.52.1.31779

Parallel Convolutional Neural Networks and Transfer Learning for Classifying Landforms in Satellite Images

Received 2022/07/05 | Accepted after revision 2022/10/08

https://doi.org/10.5755/j01.itc.52.1.31779

HOW TO CITE: Atik, I. (2023). Parallel Convolutional Neural Networks and Transfer Learning for Classifying Landforms in Satellite Images. *Information Technology and Control*, 52(1), 228-244. https://doi.org/10.5755/j01.itc.52.1.31779

Parallel Convolutional Neural Networks and Transfer Learning for Classifying Landforms in Satellite Images

Ipek Atik

Department of Electrical and Electronics Engineering, Gaziantep Islam Science and Technology University Gaziantep, 27000, Turkey; e-mail: ipek.atik@gibtu.edu.tr, ORCID ID: 0000-0002-9761-1347

Corresponding author: ipek.atik@gibtu.edu.tr

The use of remote sensing has great potential for detecting many natural differences, such as disasters, climate changes, and urban changes. Due to technological advances in imaging, remote sensing has become an increasingly popular topic. One of the significant benefits of technological advancement has been the ease with which remote sensing data is now accessible. Physical and spatial information is detected by remote sensing, which can be described as the process of identifying distinctive characteristics of an environment. Resolution is one of the most important factors influencing the success of the detection processes. As a result of the resolution being below the necessary level, features of the objects to be differentiated become incomprehensible and therefore constitute a significant barrier to differentiation. The use of deep learning methods for classifying remote sensing data has become prevalent and successful in recent years. This study classified Satellite images using deep learning and machine learning methods. Based on the transfer learning strategy, a parallel convolutional neural network (CNN) was designed in the study. To improve the feature mapping of an image, convolutional branches use pre-trained knowledge of the transmitted network. Using the offline augmentation method, the raw data set was balanced to overcome its unbalanced class distribution and increased network performance. A total of 35 classes of landforms have been studied in the experiments. The accuracy value of the developed model in the classification study of landforms was 97.84%. According to experimental results, the proposed method provides high classification accuracy in detecting landforms and outperforms existing studies.

KEYWORDS: Remote Sensing, Satellite Imagery, Transfer Learning, Machine Learning, Classification.

1. Introduction

Remote sensing is a technique introduced in the early 1960s. Compared to other images, remote sensing images are high in temporal frequency and cover wide geographical areas. As a result of the rapid developments in technology in the past years, remote sensing has become one of the most popular and important topics today. Thanks to the developing technology, the data used in the field of remote sensing has become much more accessible [17], [4]. Remote sensing can basically be called the process of detecting distinctive features such as physical or spatial information of an environment by making use of images obtained with the help of tools such as satellite vehicles, image-capable aircraft, and remote image-capable ground vehicles. In this detection process, obtaining the distinctive features of the surface or object in an accurate and workable manner is very important for applications such as analysis and object detection [34, 11, 33]. The resolution of the images obtained by the tools used in remote sensing is important. While the low resolution causes the features to become incomprehensible and indistinguishable, the situation where the resolution is above the required increases the processing load for the analyses to be made. Thanks to the increasing resolution with the developing imaging technology, the objects in the images obtained for remote sensing have become much more distinguishable and much more useful for classification [10, 22]. These conveniences in image access in remote sensing technology attract the attention of experts working on classification studies. Classification studies make great progress thanks to the data that can be accessed in the field of both modern applications and traditional applications in pixel-based examinations [40, 32]. In this area, it is possible to carry out many classification studies such as industrial structure detection, land cover classification, natural area classification, climate change detections by using remote sensing and satellite image data sets [6].

In today's technology, it has been seen that Deep Learning methods are quite successful in classifying data in the field of remote sensing. Impressive successes have been achieved in the field of successfully learning image features and obtaining suitable features for classification with deep learning methods. One of the most common deep learning methods is Convolutional Neural Networks (CNN, Convolutional Neural Network). CNN architectures have proven their suitability for classification and have been widely used in image classification and object detection in recent years [21]. When the operation of the CNN structure is examined, small, fixed size images are required to make the processing times reasonable. For this reason, operations such as size reduction in images may be necessary. In normal images, these operations can preserve important features. However, in satellite images, the situation is different from normal images because the objects and environments to be detected can be much larger than the objects and environments in ordinary images, such as an airplane on an airport runway [37].

Remote sensing and classification of satellite images are suitable for classification in many areas such as agriculture, climatic changes, disaster response and urban changes. For this reason, remote sensing is of high importance for problems and detections that require important and critical intervention. Remote sensing plays an important role in quickly detecting situations such as disasters that occur in hard-to-detect areas far from transportation [24]. There are many studies on satellite image classification in the literature. Some of these studies are summarized in Table 1.

The studies show that deep learning models have provided high performance in classification studies in recent years.

In summary, this study contributes the following novelty and main contributions:

- This study aims to conduct classification studies on satellite images used for remote sensing. The use of deep learning networks and features extracted using deep learning networks is intended to compare two different methods using machine learning algorithms and improve classification success despite the increasing number of classes.
- An effective parallel CNN model is proposed to obtain robust and high classification performance of landforms from satellite images. The proposed method combines a designed parallel structure and a transfer learning strategy.

Table 1
Studies on satellite image classification

Author	Method	Dataset	Accuracy
Dai et al. [8]	A two-layer sparse coding (TSC) model is designed to discover the real neighbors of the images and to skip the intensive learning part. K-nearest neighbor algorithms (KNN, K-nearest neighbor algorithms), Support Vector Machine (SVM) and TSC methods were applied on the data set.	For analysis, a data set was created by collecting images of 12 class labels from the Google Earth system.	It is seen that the highest success rate was obtained with the SVM method as 84.7%. It achieved a success rate of 84.2% with the TSC method.
Moorthi et al. [25]	The aim observed in the study is to compare the success between SVM and Traditional classification methods.	Resorucesat-1, LISS-3 and AWIFS sensor data from Indian Remote Sensing (IRS) platforms are used.	As a result of the analyses made, it is observed that the SVM application achieved the most successful classification result among the analyses with a success rate of 92.84%.
Xia et al. [39]	Low-level, mid-level, high-level methods (CaffeNet, VGG-VD-16, GoogLeNet) were tried on the dataset	Describes the AID dataset. More than 10,000 images were collected, and annotations were added to these images to create a comprehensive data set.	As a result of the analysis, it is observed that the highest classification success is 89.64%, using the VGG-VD-16 deep learning network.
Minu et al. [26]	It analyzes different methods of supervised classification, specific post-classification techniques, and spectral contextual classification. Aspect Comprehensive Approach (ACA) Paralelepiped, ACA Minimum Distance, Naive Bayes and K-Nearest Neighborhood algorithms were used for analysis.	It was analyzed in low and high complexity environmental images.	It is seen that the highest classification success was obtained with the ACA Paralelepiped application on images with low complexity as 89.15%.
Duarte et al. [11]	A CNN structure that considers both manned and unmanned image samples was used in the study. In the analysis, benchmark, benchmark_ft, mresA, mresB, mresC networks were used.	Images collected from Manned and UAV platforms were used.	It is seen that the highest classification success was obtained with 94.40% in the analyses made using the mresC network.
Charou et al. [7]	For the determination of agricultural and non-agricultural land, analyzes based on transfer learning are carried out with CNN and AlexNet. EuroNet, EuroNet_exp, IonioNet_PI, IonioNet_PD, IonioNet_PE2 methods were used in the study.	Democritus and EuroSAT data sets were used.	While EuroNet is the most successful classifier for EuroSAt dataset, the highest success rate for Demokritos dataset is obtained by IonioNet_PE2 classifier.
Rai et al. [28]	Principal Component Analysis (PCA) and CNN methods are presented for classification of multi-spectral satellite images using image fusion. PCA was used to reduce the size of the images.	Landsat 8 dataset was used.	In the classification process with CNN, 94.5% classification success was achieved.

Author	Method	Dataset	Accuracy
Yamashkin et al. [40]	They touched on the issue of classifying high-resolution satellite images. The main advantage of the proposed GeoSystemNet model in the study is that it is suitable for flexible configuration. In the study, many deep learning networks such as 2-layer CNN, GoogLeNet, DenseNet121, InceptionV3, ResNet50, ResNet101, VGG16, GeoSystemNet were tested.	EuroSAT data set was used.	While it is observed that the highest classification success is achieved with the InceptionV3 network with 97.93%, GeoSystemNet achieves a 95.30% success rate.
Kadhim et al. [17]	He conducted a study with the CNN structures to create systems that can handle classification without human access. AlexNet, VGG19, GoogLeNet and Resnet50 models were used in the study.	The selected models were analyzed on three different data sets, SAT4, SAT6 and UC Merced.	With the ResNet-50 model, 98% success rates for the UC Merced dataset, 95.8% for SAT4 and 94.1% for SAT6 are observed.
Pritt et al. [27]	In their studies, they discuss that detecting large geographical areas is more successful with deep learning methods compared to traditional methods.	In order to classify 63 different class labels and 57.000 images on the fMoW dataset, the CNN structure is considered.	With the CNN method used, 83% classification success was achieved, and 95% classification success was achieved on 15 of the classes.

- The method used was first tested on a 35-class data set. To test the robustness of the model, machine learning algorithms were applied on the 10-class and 20-class datasets, which were created separately, using both deep learning networks and features extracted by deep learning.
- The purpose of this application is to observe both the change in classification success according to the increase in the number of classes and the change in success rate between the pre-trained model and the proposed model.

There are five sections to this study. To contribute to previous research, the study aims to classify satellite images with CNN algorithms. The purpose of the study, its importance, and the subject of the study are discussed in the first part of the study. In the second part of the study, the material and method part, layers of convolutional neural networks, and success performance indicators of the model are discussed. The proposed CNN model used in the study is discussed in the third section, and the results are presented. In the last section, Landforms consisting of satellite images classification results are summarized and suggestions for future studies are given.

2. Material and Method

In the study, a classification study was carried out for landforms consisting of satellite images [18]. This method has 3 main steps: offline data augmentation for network improvement and transfer learning-based network training and testing [36, 31]. The dataset is randomly divided into 70% training, 15% validation and 15% test data. Each class has a different number of images in the dataset. An imbalance in the data set was avoided using the offline augmentation method. Additionally, it is used to split the data set. A training set and a validation set are used as inputs to the training, while a testing set is used for testing. The transfer learning-based network architecture is used after preprocessing to determine feature maps. The pre-trained AlexNet architecture has been enhanced with layers for transfer learning [29]. This approach learns to extract high-level features using the weight parameters of the pre-trained network and has a strong predictive ability. Figure 1 illustrates the flow chart for this classification study.

Figure 1
The general structure of the proposed classification method

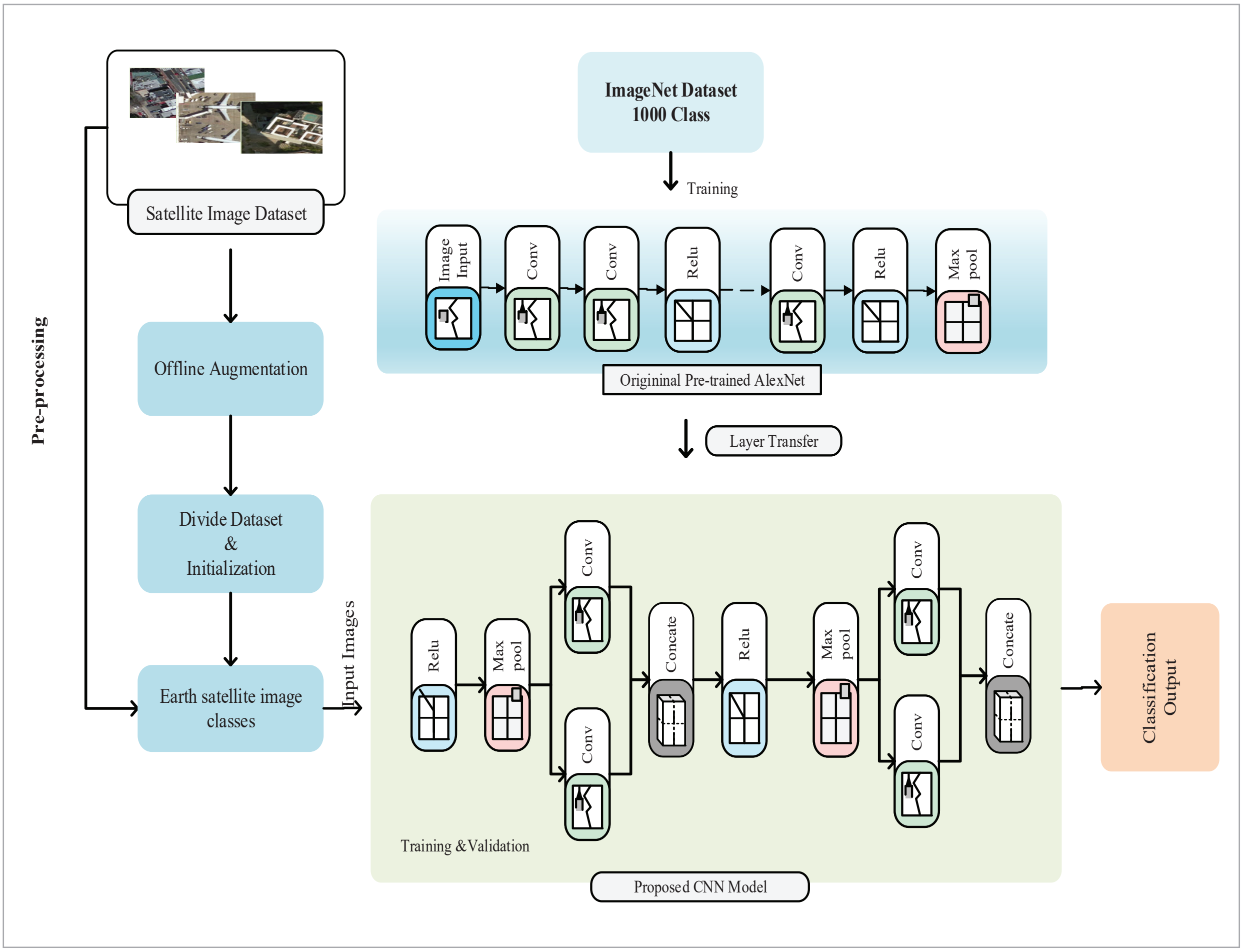

2.1. Dataset Description

The RSI-CB256 dataset, which includes publicly available satellite images, was used in the study [18]. It contains a total of 24570 images, and these images are divided into 35 classes. In the analysis, the data set was separated into 70% training, 15% validation, and 15% test data by offline augmentation. In the offline augmentation method, the data reduction process was applied to create a balanced data set. Data set visuals are as seen in Figure 2. In addition, the number of images belonging to each class is given in Table 2 [18].

2.2. Proposed Parallel CNN Model

As shown in Figure 3, the proposed CNN model is designed by modifying the AlexNet architecture and using its representation capability. AlexNet is an effective CNN model in image recognition problems offered by Alex Krishevsky et al. in the 2012 ImageNet Scale Visual Recognition Challenge (ILSVRC-2012). The original AlexNet structure consists of twelve layers with five convolution layers, three maximum pooling, three fully connected, and one classification layer. In the network, the first two convolution layers use 11×11 and 5×5, while the next three convolutions use 3×3 kernel-sized filters [19].

In the study, the pre-trained AlexNet architecture is Convolution-2, Convolution-3, Convolution-6, Convolution-8, Convolution-9, Convolution-10, Relu-2, Normalization-1, Concate-1, Concate-2, Concate-3 layers have been added. In addition, Fully Connect-6, Fully Connect-7, Fully Connect-8, Relu-6, Relu-7, Dropout 6, Dropout-7, Prop and Output layer param-

Figure 2

A sample image of each class for the satellite image data set RSI-CB256 [18]

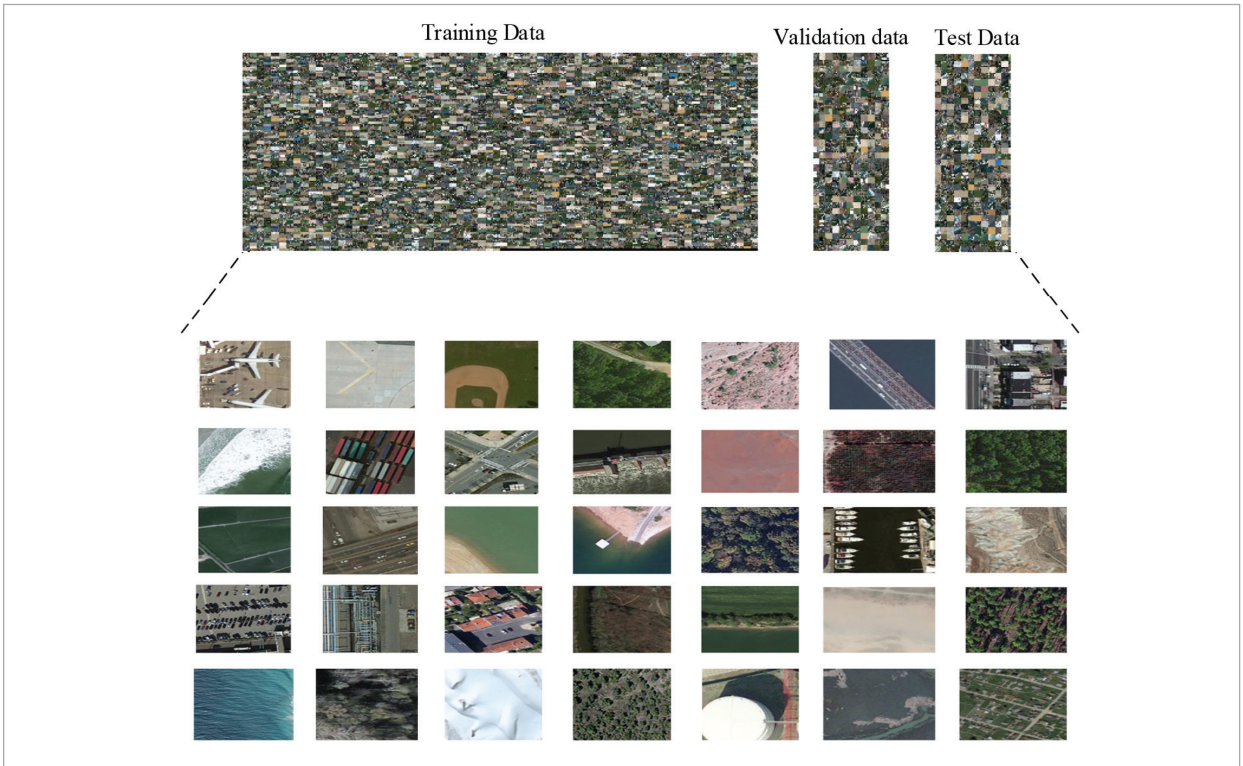

Table 2

The distribution of classes and the number of images in the dataset [18]

Classes	The number of images	Classes	The number of images
Airplane	351	Green_Farmland	644
Airport Runway	678	Highway	223
Artificial Grassland	283	Hirst	628
Avenue	544	Lakeshore	438
Bare_Land	864	Mangrove	1049
Bridge	469	Marina	366
City_Building	1014	Mountain	812
Coastline	459	Parkinglot	467
Container	660	**Pipeline**	**198**
Crossroads	553	Residents	810
Dam	324	River	539
Desert	1092	River_Protection_Forest	524
Dry_Farm	1309	Sandbeach	536
Forest	1082	Sapling	879
Sea	1028	Snow_Mountain	1153
Shrubwood	1331	Sparse_Forest	1110
Storage_Room	1307	Stream	688
Town	335		

Figure 3
The proposed cascade CNN model

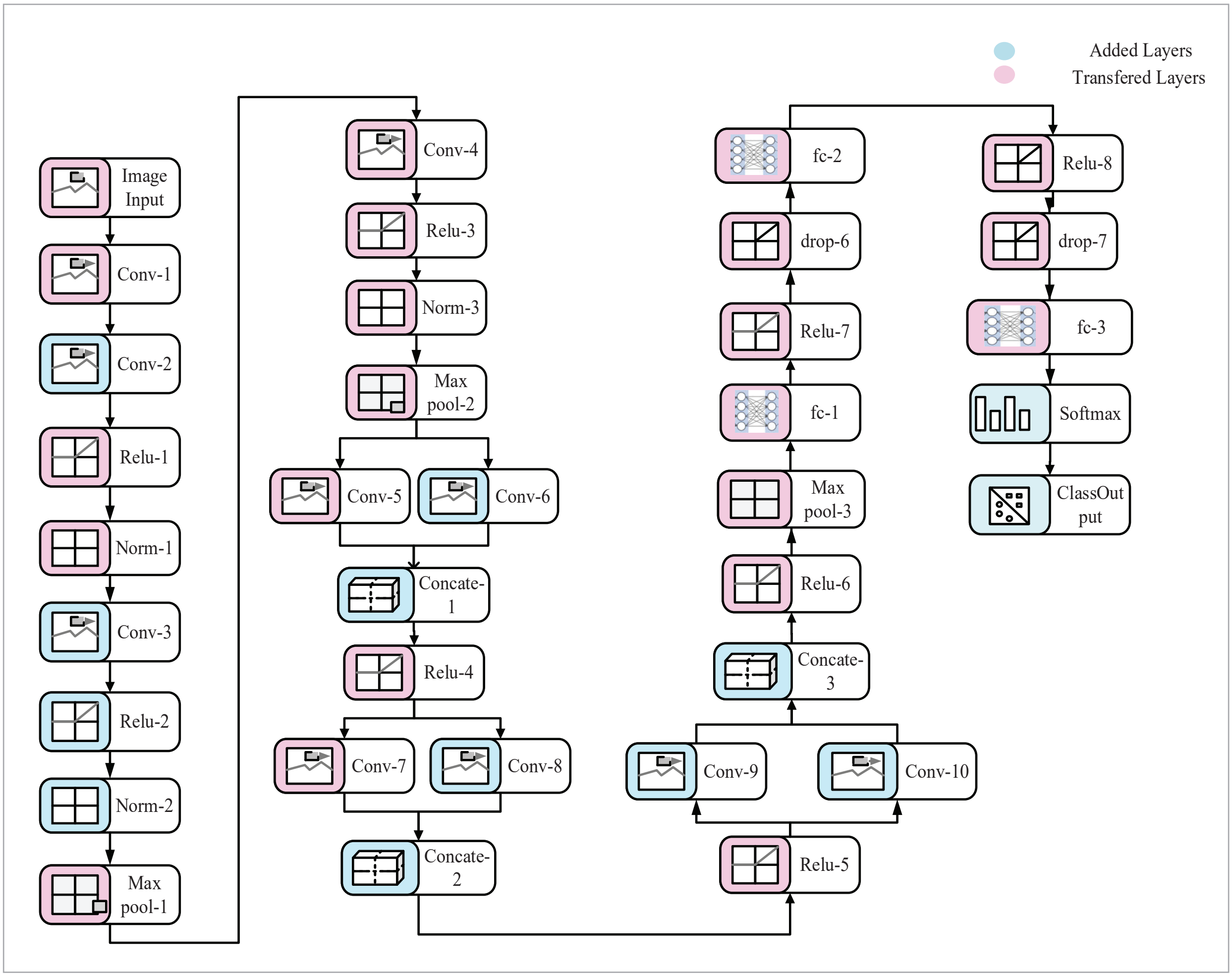

eters were re-organized in the pre-trained model. It aims to better extract the feature map of the image by combining the features from two layers in the concate layer in parallel convolution connections. An additional convolution layer is added in each of the parallel connections of the proposed parallel connected CNN model. Extraction of image features from the filtering done with the added convolution layer is provided from 2 channels. Features from each convolution layer are combined in the concate layer and transferred to the next layer. The parameters of the added layers were determined because of the experiments. Output layer parameters were chosen by the number of classes in the data set. The pre-trained AlexNet architecture and the layer relationship of the proposed model are given in Table 3. In addition, the layers added with are also indicated with Turquoise color in Figure 3. The layers in pink in Figure 3 represent the layers in the AlexNet architecture.

While the pre-trained AlexNet architecture has 25 layers, the developed model consists of 35 layers. With the parallel layers added to the model, the learning of the features of the image has increased. The model consists of 35 classes. For this reason, the depth value of fully connected 3, softmax and class output layers has been determined as 35.

2.3. Determination of Hyperparameter Value Intervals

Determining the optimum hyperparameter values in CNN model training is determined depending on the data set, the size of the data set and the model. Accord-

Table 3
Relationship between the proposed model and AlexNet architecture

Alexnet	Proposed Model	Description	Depth
Conv-1	Conv_1	Transferred layer	96
-	Conv_2	Adding new layer	96
Relu_1	Relu_1	Transferred layer	96
Norm_1	Norm_1	Transferred layer	96
-	Conv_3	Adding new layer	96
-	Relu_2	Adding new layer	96
-	Norm_2	Adding new layer	96
Maxpool_1	Maxpool_1	transferred layer	96
Conv_2	Conv_4	transferred layer	256
Relu_2	Relu_3	transferred layers	256
Norm_2	Norm_2	transferred layer	256
Maxpool_2	Maxpool_2	transferred layer	256
Conv_3	Conv_5 Conv_6	Adding new layer	384
-	Concate_1	Adding new layer	384
Relu_3	Relu_4	transferred layers	384
Conv_4	Conv_7 Conv_8	Adding new layer	384
-	Concate_2	Adding new layer	384
Relu_4	Relu_5	transferred layers	384
Conv_5	Conv_9 Conv_10	Adding new layer	256
-	Concate_3	Adding new layer	256
Relu_5	Relu_6	transferred layer	256
Maxpool_5	Maxpool_5	transferred layer	256
Fc_6	Fc_1	transferred and re-organize layer	1024
Relu_6	Relu_7	transferred and re-organize layer	1024
Drop_6	Drop_6	transferred and re-organize layer	1024
Fc-7	Fc_2	transferred and re-organize layer	1024
Relu_7	Relu_8	transferred and re-organize layer	1024
Drop_7	Drop_7	transferred and re-organize layer	1024
Fc_8	Fc_3	transferred and re-organize layer	35
Prop	Softmax	transferred and re-organize layer	35
Output	Class Output	transferred and re-organize layer	35

ing to the literature research, some of the implications regarding educational hyperparameters are given below.

The mini-batch size is used to process all data in small batches to improve network performance and use memory. It means how much data the model will process simultaneously. The larger mini-batch size requires more memory, while the smaller mini-batch size causes more noise in error calculation [20].

Appropriate hyperparameter selection has an important place in deep learning architecture. Optimization parameters such as learning rate, mini-batch size, and several epochs and unique model parameters such as activation functions, dropout value, and several layers are among the parameters that affect the CNN result. The learning rate can be set to a fixed value or a certain level, increasing or decreasing. Generally, the learning rate is chosen between 0.1 and 0.000001. Choosing this value too low or too high will adversely affect the model. If it is too small than the optimum value, it will take a long time to reach the ideal deal. If it is too large, the excellent value may be exceeded, and the model may never get perfect weight. A learning rate that can reach and catch the superb value should be chosen without being stuck with the local minimum value. The mini batch size can be set to 32, 64, 128, and 256 [12, 5]. All analyzes were determined as drop factor 0.7, drop period is 10, and the weight decay is 0.0001.

Stochastic gradient descent with momentum (SGDM) algorithm was used as the optimization algorithm. The SGDM used in the training period accelerates the gradient vectors in the right directions and tries to find the minimum or maximum with iterations. The epoch number is one complete model revolution from start to finish. A low number of epochs may cause the under-learning of the model, while over-selecting it may cause over-learning of the model. The dropout layer is used to prevent the network from memorizing during training [16, 1]. The most appropriate hyperparameter ranges used in this study were determined by considering the dataset, CNN architecture and the size of the dataset, given in Table 5.

3. Experiments

In this part of the study, the statistical validity of the proposed method was analyzed with experimental methods. Experimental studies were carried out in MATLAB® R2020b environment and on Intel (R) Core™ i7-10750H CPU @2.60 GHz, NVIDIA Quadro P620 GPU 16 GB RAM, and x64 based processor. The following section provides definitions of evaluation criteria. In addition, experimental and improvement studies were carried out in the next section. Finally, the performance of the proposed method is compared with the state-of-the-art techniques.

3.1. Evaluation Metrics

Machine learning uses a confusion matrix for performance measurement in classification studies. The confusion matrix is a table containing four different predicted and actual value combinations. An example confusion matrix is given in Table 4.

In Table 4 given classes m, a $CM_{i,j}$ entry in a confusion matrix represents the number of tuples in class i labeled as class j by the classifier. For a classifier to have good accuracy, ideally most of the tubles are represented along the diagonal of the confusion matrix from the $CM_{1,1}$ input to the $CM_{m,m}$ input, with the rest of the inputs zero or near zero. There are some metrics we can calculate with these terms [38, 2, 13].

Table 4

Illustration of a confusion matrix [3]

Predicted Class / Actual Class	C_1	C_2	...	C_m	Total
C_1	$CM_{1,1}$	$CM_{1,2}$	...	$CM_{1,m}$	AC_1
C_2	$CM_{2,1}$	$CM_{2,2}$	...	$CM_{2,m}$	AC_2
. . .			...		
C_m	$CM_{m,1}$	$CM_{m,2}$	...	$CM_{m,m}$	AC_m
Total	PC_1	PC_2		PC_m	AC_1 +...+AC_m

Accuracy (Acc) is the percentage of samples correctly classified. Sensitivity (Sn) or Recall is a metric that shows how many transactions we need to predict and what we expect positively. Precision shows how many of the values we predicted as positive are positive. Specificity (Sp) the actual Positive Rate corresponds to the proportion of positive data points considered positive concerning all positive data points. The f score (f1) measures the accuracy of a test—the harmonic means of precision and sensitivity. These terminologies showing the relationships are given in Equations (1)-(5) [15].

$$Accuracy = \frac{\sum_i CM_{i,i}}{\sum_j \sum_i CM_{i,j}} \tag{1}$$

$$Error\ Rate = 1 - Accuracy \tag{2}$$

$$Precision_{C_i} = \frac{CM_{i,i}}{\sum_j CM_{j,i}} \tag{3}$$

$$Recall_{C_i} = \frac{CM_{i,i}}{\sum_j CM_{i,j}} \tag{4}$$

$$F1 = \frac{2 \times Precision \times Recall}{Precision + Recall}. \tag{5}$$

The above metrics can analyze the proposed method's accuracy, efficiency, and robustness [9, 30, 35, 23, 14].

3.2. Experimental Results

This study comprises 35 classes and 24570 satellite images [18]. Each image is 256 by 256 pixels. The image dimensions for model inputs are resized according to the dimensions of the model inputs. It is divided into a training dataset of 70%, a validation dataset of 15%, and a test dataset of 15%.

In the classification studies with machine learning, the unbalanced class distribution in the data set negatively affects the model performance. The data set was balanced with the offline augmentation method. The class with the least number of images was determined, and many images were taken randomly from all classes.

Pipeline class with 198 images is the class with the least number of images among 35 classes during the training phase. In the analysis, 198 images were taken randomly from each class and a balanced data set consisting of a total of 6930 images was created. 70% of this data set was taken as training, 15% as validation and 15% as test data.

Table 5
Hyperparameters for CNN models

Parameter	Value
Mini batch size	16
Max. period	100
Initial learning rate	$1e^{-4}$
Optimization	sgdm

A total of 4851 images of training data are given to the network for training. The feature maps of the images were extracted, and the dataset of the network was learned. With the validation data set created, the network is prevented from memorizing. The performance of the network was evaluated with the test data that was not given to the network before.

During determining the hyperparameters, the model has been fine-tuned to enhance performance. Based on the results of the experiments, the hyperparameters listed in Table 5 were preferred.

The accuracy rate and training loss values of the proposed model and the AlexNet model during the training period are given in Figure 4. The high accuracy of

Figure 4
Training progress of the AlexNet and proposed parallel CNN experiments

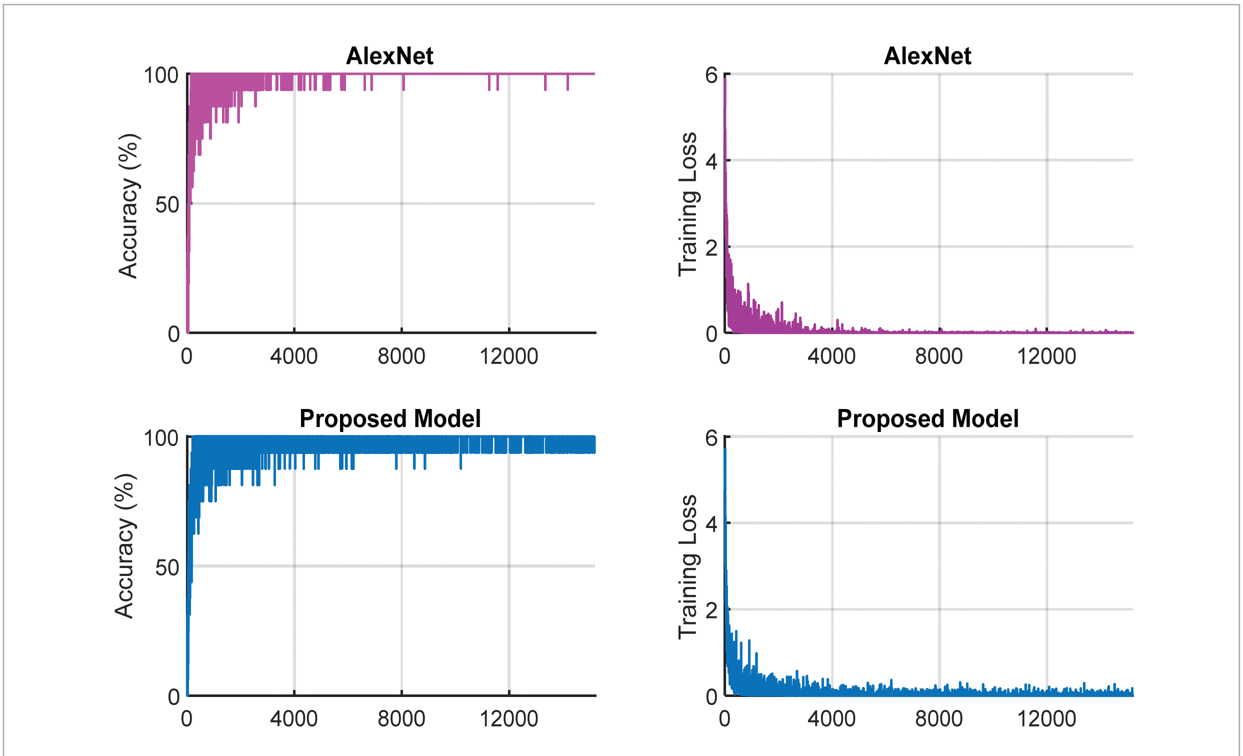

the model indicates that the network has learned the properties of the images well. The training time varies depending on the number of epochs.

A confusion matrix is a table used to describe the performance of a classification model on a set of test data for which actual values are known. Figure 5 shows confusion matrices for the proposed model on test data. In the classification estimation study, 29 test images were used for each class. When the proposed model analyzed the confusion matrix, it was found that it could not correctly predict the class of 22 images. Airplane, Air-port Runway, Artificial Grassland Hirst, Container, Dry_Farm, Forest, Mangrove, Marina, Mountain, Parking lot, Pipeline, River_Protection_Forest, Sandbeach, Sapling, Sea, Shrubwood, Snow_Mountain, Sparse_Forest, Storage_Room, Stream, Town and predicted 29 images in the correct classes. Only one was incorrectly guessed among the images in the Avenue, Crossroads, Dam, Green_Farmland, Highway, and River classes. However, two of the test images belonging to the Lakeshore, Bare_Land, Bridge City_Building, Coastline, Residents, and Desert classes could not correctly predict the class of the images. While the analysis made with AlexNet architecture took 76 minutes, the proposed parallel connected CNN model analysis time was 78 minutes.

One of the expressions used when evaluating the classification performance of the model is the ROC (Receiver Operating Characteristics) curve method. The ROC curve is the graph of the ratio of the cor-

Figure 5

Proposed model confusion matrix results for 35 classes

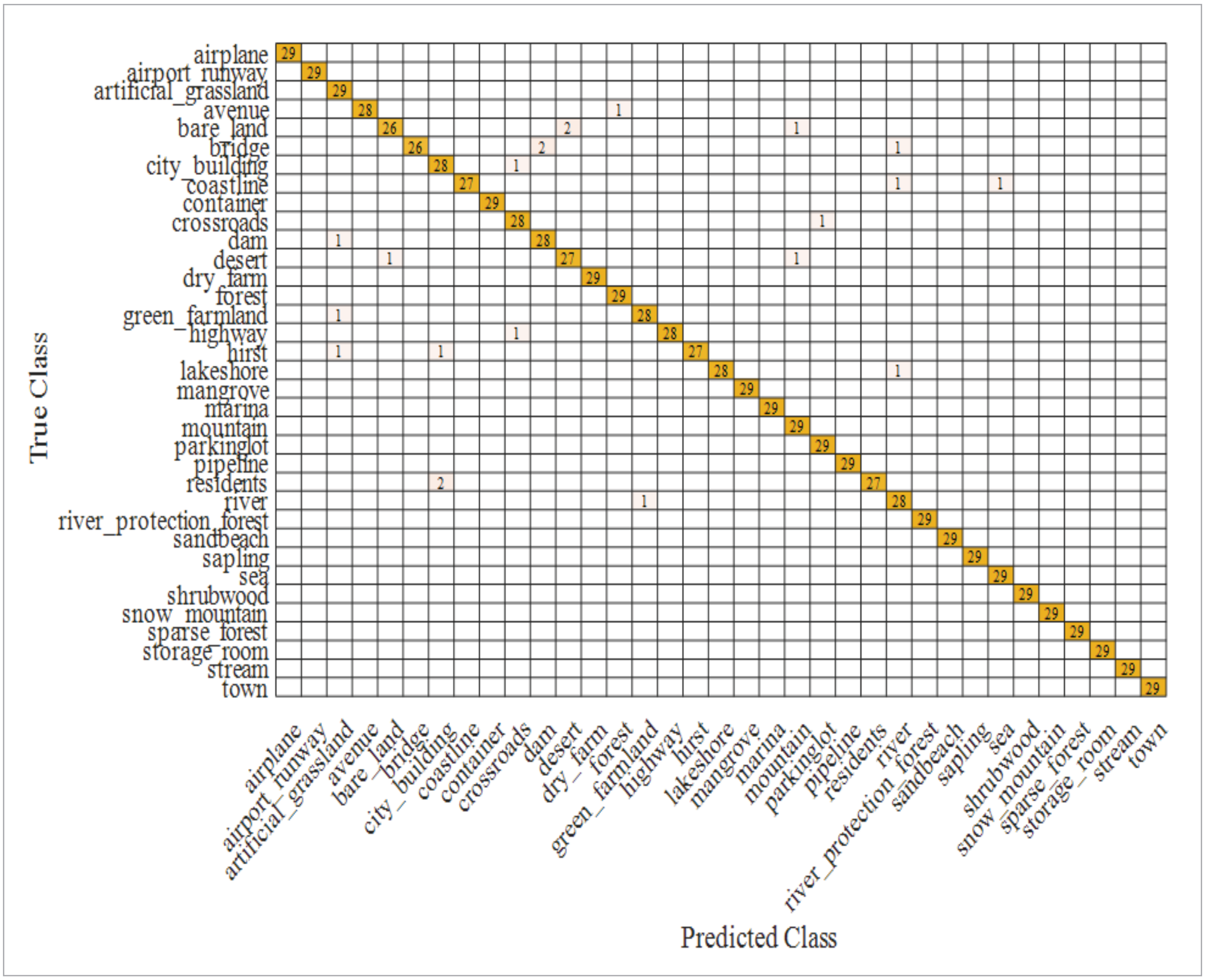

Figure 6
ROC curve for the 35-class dataset of the proposed model

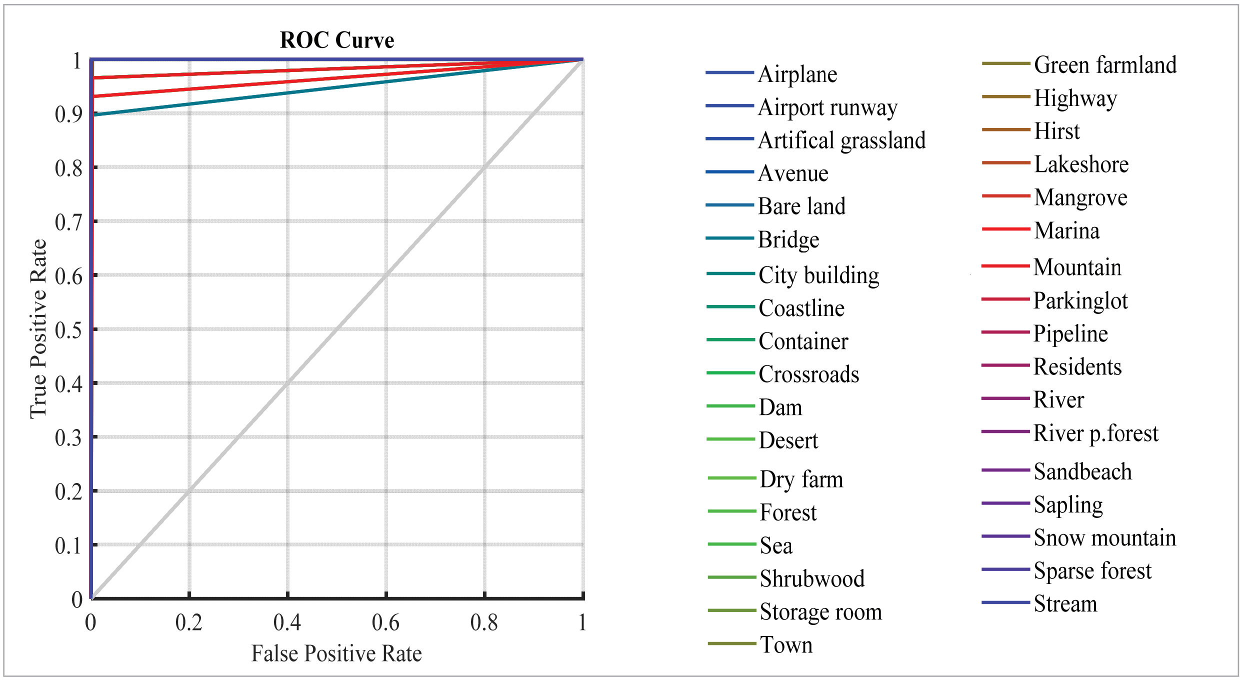

rect positive rate (sensitivity) and false positive rate (1-specificity) parameters. When the ROC score is 1 (one), the positives are perfectly separated from the negatives, and when the ROC score is 0 (zero), it is deduced that no positives can be found. ROC curves of bad, good and very good (excellent) performance tests are given in Figure 6 (Hoo, Candlish, & Teare, 2017).

In the analysis that is perfect on the ROC curve, the curve passes through the points (0,0), (0,1) and (1,1). A bad ROC curve is diagonal from (0,0) to (1.1). The result of the analysis is evaluated according to these two curves.

Activations of the proposed method in different convolutions are given in Figure 7. Conv-1 and Conv-3 rep-

Figure 7
Activations from different convolutions

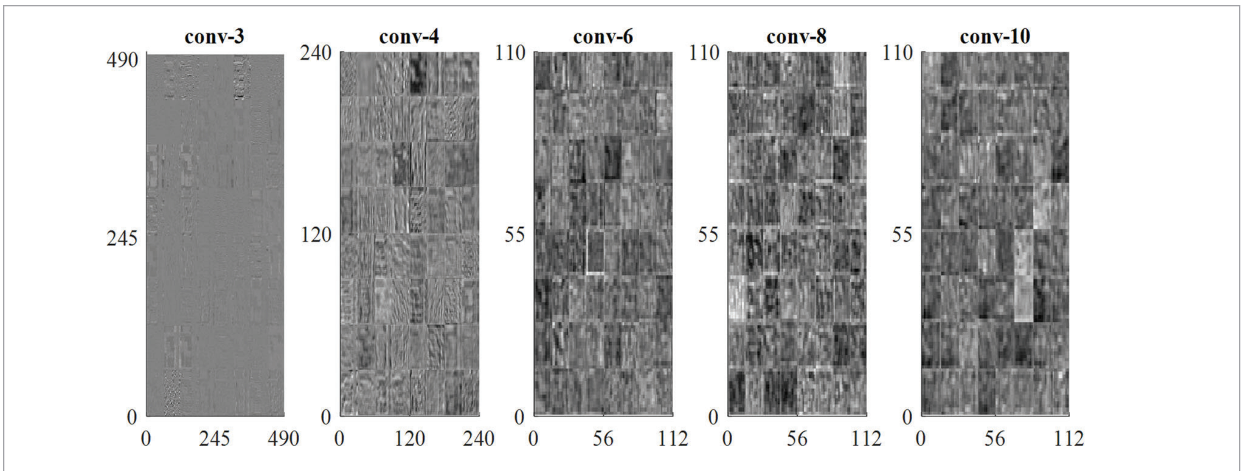

resent the first two convolutions, while Conv 6-8-10 represent parallel branches. By comparing the original input image with the activation fields, the features the proposed method has learned can easily be obtained. White pixels indicate strong positive activations, and black pixels indicate strong negative activations. Additionally, white pixels in a channel identify the strongly activated channel at that location.

Figure 8 shows the t-distributed stochastic neighbor insertion. T-Distributed Stochastic (Random) Neighbor Embedding (t-SNE); It is an unsupervised, non-linear technique used primarily for the exploration and visualization of high-dimensional data. It calculates the probability that pairs of data points in high-dimensional space are related and then chooses a low-dimensional embedding that produces a simi-

Figure 8

The t-SNE view of the features extracted from the convolution layers of the proposed method

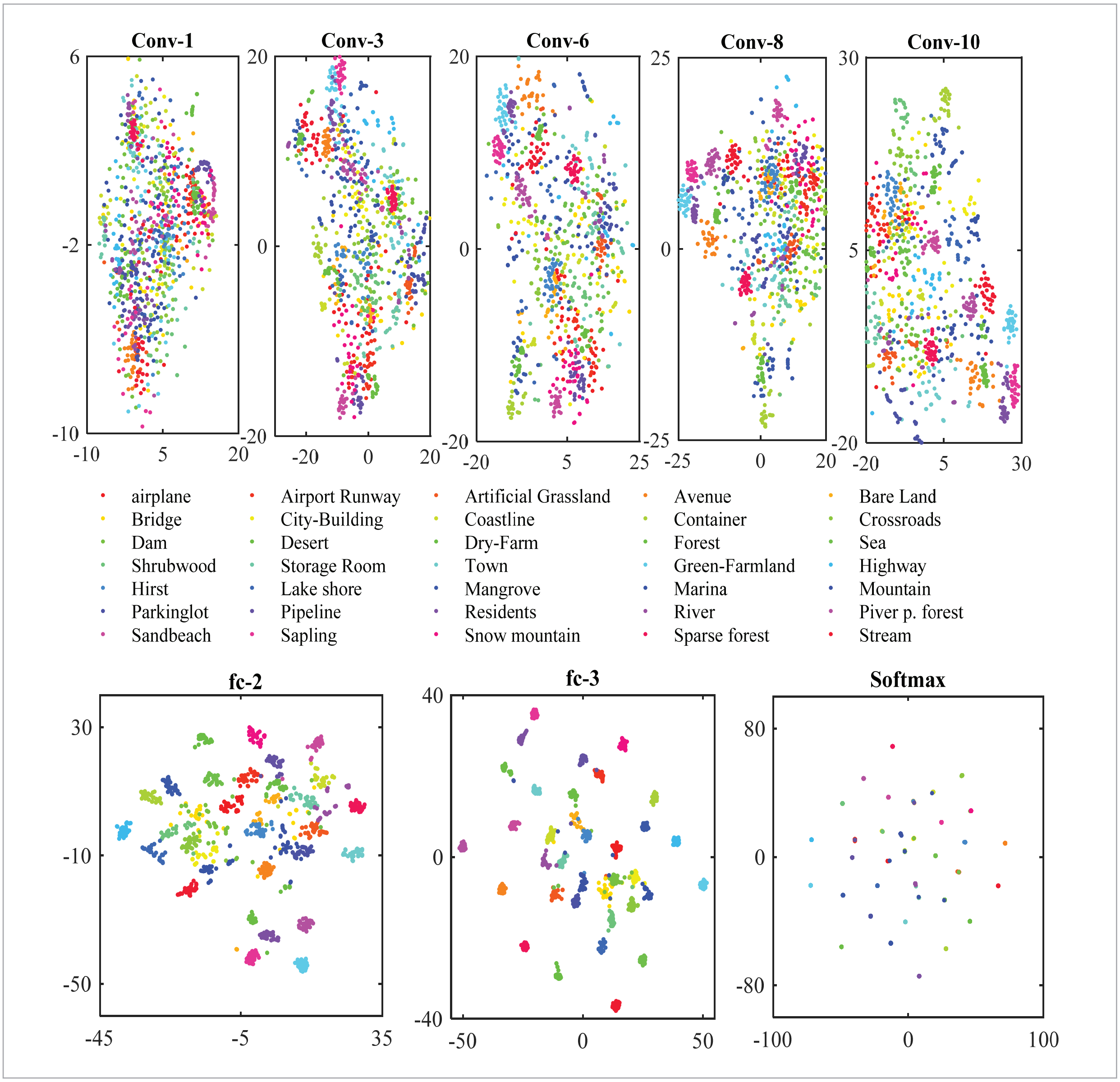

lar distribution. The T-SNE algorithm calculates the similarity measure between pairs of samples in high and low dimensional space. According to the clusters made according to the feature maps in Figure 8, while it is complex in the first layers, the maps in the last layers are clustered in separate regions for each class. When the clusters in the SoftMax layer, which is the final layer of the proposed method, are analyzed, it is seen that the distribution of the classes is quite good

3.3. Performance Testing of the Proposed Model with Different Datasets

To test the performance of the model proposed in the study with different data sets, balanced data sets with 10 classes and 20 classes consisting of landforms were created. The data sets were balanced to make the correct analysis in the analyses. 70% of the images are reserved as training, 15% validation and 15% test data. In the analyses, the hyperparameters values were chosen the same as the values given in Table 5.

Confusion matrices obtained from the analysis of the proposed model with 10-class and 20-class data sets are given in Figure 9 and Figure 10, respectively. As a result of the data sets analysis, the performance metrics values were obtained as seen in Table 6.

Figure 9

Proposed model confusion matrix results for 10 classes

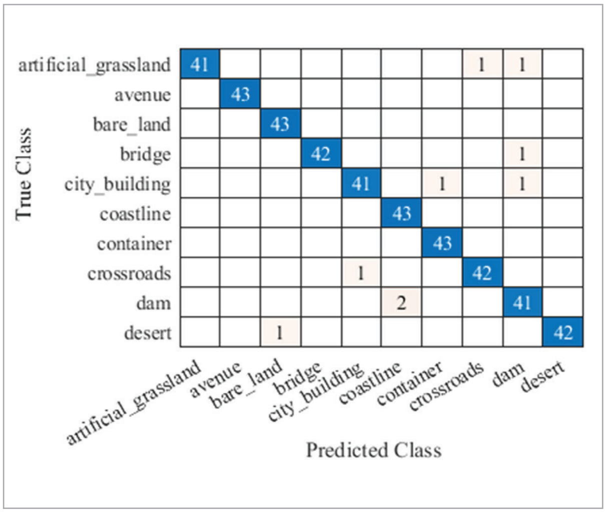

Figure 10

Proposed model confusion matrix results for 20 classes

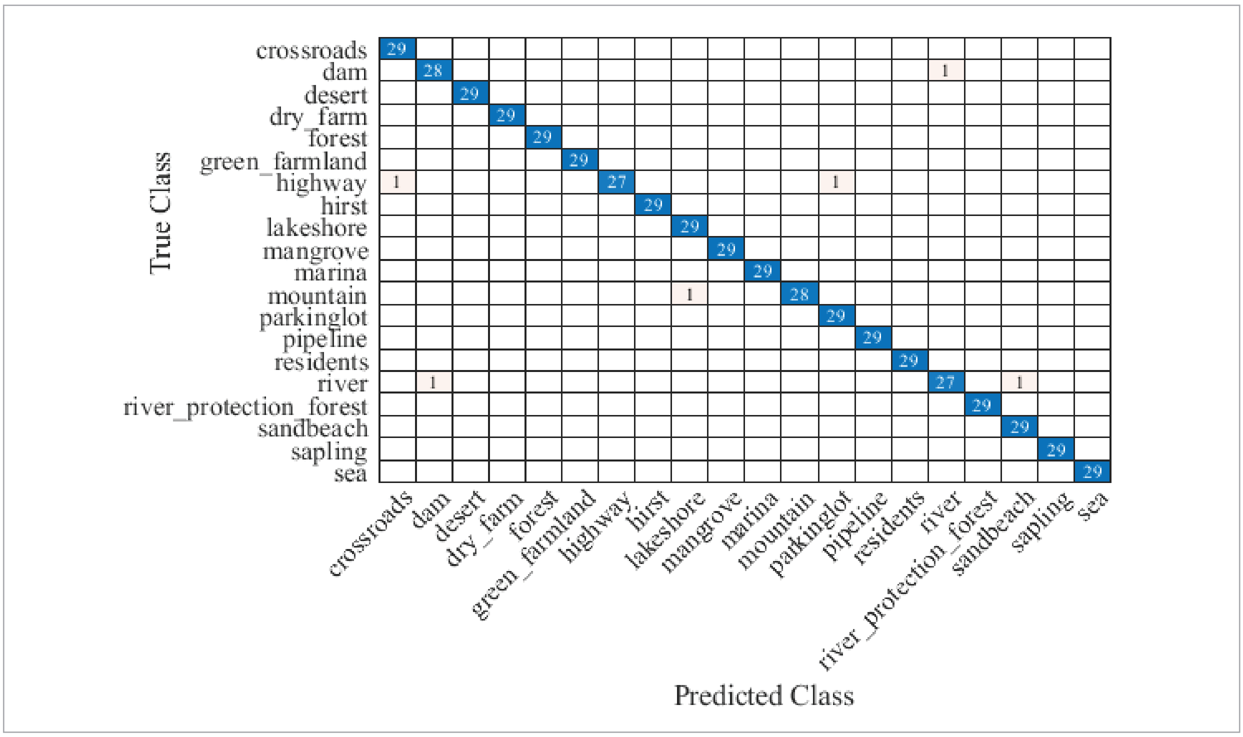

Table 6
Performance comparison of different datasets (%)

Number of Dataset Classes	Model	Acc	Sp	Sn	Pr	F1
10 Classes	AlexNet	96.98	99.66	96.98	96.98	96.97
	Proposed model	97.91	99.77	97.91	97.95	97.91
20 Classes	AlexNet	97.93	99.89	97.93	98.06	97.95
	Proposed model	98.97	99.95	98.97	98.98	98.96
35 Classes	AlexNet	96.45	99.90	96.45	96.57	96.43
	Proposed model	97.84	99.94	97.83	97.93	97.82

As a result of the 35-class dataset analyses, the accuracy, specificity, sensitivity, precision, and f1-score values of the proposed parallel CNN model were obtained as 97.84%, 99.94%, 97.83%, 97.93%, and 97.82%, respectively. Analyses were also performed for pre-trained AlexNet using the same hyperparameters with the same data to evaluate model performance. Accuracy, specificity, sensitivity, precision, and f-score values in the AlexNet model were obtained as 96.45%, 99.90%, 96.45%, 96.57%, and 96.43%, respectively.

Accuracy values for 10-class and 20-class data sets were obtained as 97.91% and 98.97%, respectively. The specifity, sensitivity, precision and f-score values for the 10-class dataset were obtained as 99.77%, 97.91%, 97.95% and 97.91%, respectively. The specifity, sensitivity, precision and f-score values for the 20-class dataset were obtained as 99.95%, 98.97%, 98.98% and 98.96%, respectively.

When the 10-class and 20-class dataset performance metric results are compared with the 35-class dataset analysis performance results, it is seen that the best performance is obtained with the 20-class dataset.

AlexNet, which is important for our study, and the proposed model were tested on different data sets, and the proposed model showed higher performance than AlexNet in all three different data sets.

4. Conclusions

A powerful deep learning model is proposed in this study. The study categorizes 35 classes of landforms from satellite images. Due to the excess of some landform images, the offline augmentation method stabilizes the data set. In this way, the model performance has increased. The developed parallel CNN model is compared with the pre-trained AlexNet model. The AlexNet model obtained accuracy, specificity, sensitivity, precision, and f-score values as 96.45%, 99.90%, 96.45%, 96.57%, and 96.43%, respectively. It is seen that the proposed parallel CNN model improves the accuracy by 1.44%. The proposed CNN model's accuracy, specificity, sensitivity, precision, and f-score values were obtained as 97.84%, 99.94%, 97.83%, 97.93%, and 97.82%, respectively. It is seen that the proposed model improves accuracy, specificity, sensitivity, precision, and f-score by 1.43%, 0.04%, 1.43%, 1.41%, and 1.46%, respectively.

In future studies, optimization algorithms can be developed to improve the classification performance of the CNN model. It can be used in the classification of landforms for data sets belonging to a different number of classes.

References

1. Atik, I. Classification of Electronic Components Based on Convolutional Neural Network Architecture. Energies, 2022, 15(7), 2347. https://doi.org/10.3390/en15072347
2. Atik, I. Performance Comparison of Pre-Trained Convolutional Neural Networks in Flower Image Classification. European Journal of Science and Technology, 2022, 35, 315-321.

3. Atik, I. A New CNN-Based Method for Short-Term Forecasting of Electrical Energy Consumption in the Covid-19 Period: The Case of Turkey. IEEE Access, 2022, 10, 22586-22598. https://doi.org/10.1109/ACCESS.2022.3154044
4. Aydemir, C. Classification of Satellite Images with Deep Learning and Machine Learning. Başkent University Institute of Science and Engineering Department of Electrical and Electronics Engineering, 2022.
5. Banerjee, B., Bovolo, F., Bhattacharya, A., Bruzzone, L., Chaudhuri, S., Mohan, B. K. A New Self-Training-Based Unsupervised Satellite Image Classification Technique Using Cluster Ensemble Strategy. IEEE Geoscience and Remote Sensing Letters, 2015, 12(4), 741-745. https://doi.org/10.1109/LGRS.2014.2360833
6. Castelluccio, M., Poggi, G., Sansone, C., Verdoliva, L. Land Use Classification in Remote Sensing Images by Convolutional Neural Networks. arXiv:1508.00092v1
7. Charou, E., Felekis, G., Stavroulopoulou, D. B., Koutsoukou, M., Panagiotopoulou, A., Voutos, Y., Bratsolis, E., Mylonas, P., Likforman-Sulem, L. Deep Learning for Agricultural Land Detection in Insular Areas. 10th International Conference on Information, Intelligence, Systems and Applications (IISA), 2019, 1-4. https://doi.org/10.1109/IISA.2019.8900670
8. Dai, D., Yang, W. Satellite Image Classification Via Two-layer Sparse Coding with Biased Image Representation. IEEE Geoscience and Remote Sensing Letters, 2010, 8(1), 173-176. https://doi.org/10.1109/LGRS.2010.2055033
9. Deng, L., Yu, D. Deep Learning: Methods and Applications. Found Trends Signal Process, 2014, 7(3-4), 197-387. https://doi.org/10.1561/2000000039
10. Doğan, F., Turkoglu, I. Classification of Satellite Images by Deep Learning, 2021.
11. Duarte, D., Nex, F., Kerle, N., Vosselman, G. Satellite Image Classification of Building Damages Using Airborne and Sa TEL Lite Image Samples in a Deep Learning Approach. ISPRS Annals of the Photogrammetry, Remote Sensing and Spatial Information Sciences, 2018, IV-2, 89-96. https://doi.org/10.5194/isprs-annals-IV-2-89-2018
12. Fassnacht, F. E., Neumann, C., Förster, M., Buddenbaum, H., Ghosh, A., Clasen, A., Joshi, P. K., Koch, B. Comparison of Feature Reduction Algorithms for Classifying Tree Species with Hyperspectral Data on Three Central European Test Sites. IEEE Journal of Selected Topics in Applied Earth Observations and Remote Sensing, 2014, 7(6), 2547-2561. https://doi.org/10.1109/JSTARS.2014.2329390
13. Fausett, L. Fundamentals of Neural Networks: Architectures, Algorithms, and Applications. USA: Prentice-Hall, Inc., 1994.
14. Guyet, T., Nicolas, H. Long Term Analysis of Time Series of Satellite Images. Pattern Recognition Letters, 2015, 70. https://doi.org/10.1016/j.patrec.2015.11.005
15. Hinton, G., Osindero, S., Teh, Y.-W. A Fast Learning Algorithm for Deep Belief Nets. Neural Computation, 2006, 18, 1527-54. https://doi.org/10.1162/neco.2006.18.7.1527
16. Hussain, M., Bird, J. J., Faria, D. R. A Study on CNN Transfer Learning for Image Classification. Advances in Computational Intelligence Systems, Cham, 2019, 191-202. https://doi.org/10.1007/978-3-319-97982-3_16
17. Kadhim, M., Abed, M. Convolutional Neural Network for Satellite Image Classification. In Studies in Computational Intelligence, 2020, 165-178. https://doi.org/10.1007/978-3-030-14132-5_13
18. Kaggle data set, 06-Dec-2021. [Online]. Available: https://www.kaggle.com/datasets.
19. Krizhevsky, A., Sutskever, I., Hinton, G. E. Imagenet Classification with Deep Convolutional Neural Networks. Advances in Neural Information Processing Systems, 2012, 25, 1097-1105.
20. LeCun, Y., Bengio, Y., Hinton, G. Deep Learning. Nature, 2015, 521, 436-44. https://doi.org/10.1038/nature14539
21. Liu, Q., Basu, S., Ganguly, S., Mukhopadhyay, S., DiBiano, R., Karki, M., Nemani, R. R. DeepSat V2: Feature Augmented Convolutional Neural Nets for Satellite Image Classification. CoRR, 2019, vol. abs/1911.07747. https://doi.org/10.1080/2150704X.2019.1693071
22. Maggiori, E., Tarabalka, Y., Charpiat, G., Alliez, P. Recurrent Neural Networks to Enhance Satellite Image Classification Maps. CoRR, vol. abs/1608.03440, 2016.
23. Matworks, «Pretrained Deep Neural Networks.» Matworks.
24. Michie, D., Spiegelhalter, D., Taylor, C. Machine Learning, Neural and Statistical Classification. Technometrics, 1999, 37.
25. Moorthi, S. M., Misra, I., Kaur, R., Darji, N. P., Ramakrishnan, R. Kernel Based Learning Approach for Satellite Image Classification Using Support Vector Machine. 2011 IEEE Recent Advances in Intelligent Computational Systems, 2011, 107-110.

26. Nair, M., B. J. S. Supervised Techniques and Approaches for Satellite Image Classification. International Journal of Computer Applications, 2016, 134, 1-6. https://doi.org/10.5120/ijca2016908202
27. Pritt, M., Chern, G. Satellite Image Classification with Deep Learning. arXiv:2010.06497, 2017, 1-7. https://doi.org/10.1109/AIPR.2017.8457969
28. Rai, A. K., Mandal, N., Singh, A., Singh, K. K. Landsat 8 OLI Satellite Image Classification Using Convolutional Neural Network. Procedia Computer Science, 2020, 167, 987-993. https://doi.org/10.1016/j.procs.2020.03.398
29. Romero, A., Gatta, C., Camps Valls, G. Unsupervised Deep Feature Extraction for Remote Sensing Image Classification. IEEE Transactions on Geoscience and Remote Sensing, 2016, 54, 1349-1362. https://doi.org/10.1109/TGRS.2015.2478379
30. Schmidhuber, J. Deep Learning in Neural Networks: An Overview. CoRR, 2014, abs/1404.7828.
31. Scott, G. J., England, M., Starms, W. A., Marcum, R. A., Davis, C. H. Training Deep Convolutional Neural Networks for Lan. Cover Classification of High-Resolution Imagery. I IEEE Transactions on Geoscience and Remote Sensing, 2017, 14, 549-553. https://doi.org/10.1109/LGRS.2017.2657778
32. Tammina, S. Transfer Learning Using VGG-16 with Deep Convolutional Neural Network for Classifying Images. International Journal of Scientific and Research Publication, 2019, 9, 9420. https://doi.org/10.29322/IJSRP.9.10.2019.p9420
33. Tonyaloğlu, E. E., Erdogan, N., Çavdar, B., Kurtşan, K., Nurlu, E. Comparison of Pixel and Object Based Classification Methods on Rapideye Satellite Image. Turkish Journal of Medical Sciences, 2021, 5(1), 1-11. https://doi.org/10.32328/turkjforsci.741030
34. Tout, K., Yassine, H., Jaber, M. Improving LULC Classification from Satellite Imagery Using Deep Learning - Eurosat Dataset, 2021.
35. Ucar, F., Alcin, O., Dandil, B., Ata, F. A Novel Classification Method Based on One Dimensional Local Binary Patterns and Discrete Wavelet Transform for Power Quality Events. Kahramanmaras Sutcu Imam University Journal of Engineering Sciences, 2016, 7-13.
36. Unnikrishnan, A., S. V, S. K. P. Deep AlexNet with Reduced Number of Trainable Parameters for Satellite Image Classification. Procedia Computer Science, 2018, 143, 931-938. https://doi.org/10.1016/j.procs.2018.10.342
37. Verde, N., Mallinis, G., Tsakiri-Strati, M., Georgiadis, C., Patias, P. Assessment of Radiometric Resolution Impact on Remote Sensing Data Classification Accuracy. Remote Sens., vol. 10, no. 8, 2018. https://doi.org/10.3390/rs10081267
38. Voigt, S., Kemper, T., Riedlinger, T., Kiefl, R., Scholte, K., Mehl, H. Satellite Image Analysis for Disaster and Crisis-management Support. IEEE Transactions on Geoscience and Remote Sensing, 2007, 45(6), 1520-1528. https://doi.org/10.1109/TGRS.2007.895830
39. Xia, G.-S., Hu, J., Hu, F., Shi, B., Bai, X., Zhong, Y., Zhang, L., Lu, X. AID: A Benchmark Data Set for Performance Evaluation of Aerial Scene Classification," IEEE Geoscience and Remote Sensing Letters, 2017, 55(7), 3965-3981. https://doi.org/10.1109/TGRS.2017.2685945
40. Yamashkin, S. A., Yamashkin, A. A., Zanozin, V. V., Radovanovic, M. M., Barmin, A. N. Improving the Efficiency of Deep Learning Methods in Remote Sensing Data Analysis: Geosystem Approach. IEEE Access, 2020, 8, 179516-179529. https://doi.org/10.1109/ACCESS.2020.3028030